**Glycobiology** vol. 17 no. 3 pp. 261–276, 2007
doi:10.1093/glycob/cwl076
Advance Access publication on December 15, 2006

# Developmental changes in the expression of glycogenes and the content of *N*-glycans in the mouse cerebral cortex

**Akihiro Ishii[2,3*], Takeshi Ikeda[2,3*], Seiji Hitoshi[2,3], Ichiro Fujimoto[2,3], Tomohiro Torii[2,3], Keiichiro Sakuma[3], Shin-ichi Nakakita[4], Sumihiro Hase[5], and Kazuhiro Ikenaka[1,2,3]**

[2]Department of Physiological Sciences, The Graduate University for Advanced Studies (SOKENDAI), Okazaki, Aichi 444-8585, Japan; [3]Division of Neurobiology and Bioinformatics, National Institute for Physiological Sciences, Institutes of Natural Sciences, 5-1 Higashiyama, Myodaiji, Okazaki, Aichi 444-8787, Japan; [4]Department of Functional Glycomics, Life Science Research Center, Kagawa University, 1750-1 Ikenobe, Miki-cho, Kita-gun, Kagawa 761-0793, Japan; and [5]Department of Chemistry, Graduate School of Science, Osaka University, Osaka 560-0043, Japan

*Received on May 10, 2006; revised on November 23, 2006; accepted on December 1, 2006*

**Biosynthesis of *N*-glycans varies significantly among tissues and is strictly regulated spatially and temporally within the tissue. The strict molecular mechanisms that are responsible for control of *N*-glycan synthesis remain largely unknown. We developed complementary deoxyribonucleic acid (cDNA) macroarray system and analyzed gene expression levels of more than 140 glycosyltransferases and glycosidases in the cerebral cortex from developing and adult mice. We also analyzed the relative amounts of major *N*-glycans present in the cerebral cortex and examined how the synthesis of *N*-glycans might be regulated through the expression of these genes. We demonstrated that the content of *N*-linked oligosaccharides dramatically changed during the course of brain development. Some of these changes could not be explained by alterations in the expression of the corresponding genes. For example, the amount of core fucosylated sugar chains in the early embryonic brain and the expression level of fucosyltransferase VIII, the only gene known to be responsible for core fucosylation, did not change proportionately. This result suggests that post-transcriptional regulation of this gene plays an important role in regulating its enzymatic activity. On the other hand, the amount of β1,3-galactose residue-containing sugar chains increased postnatally following an increase in the level of β1,3-galactosyltransferase messenger ribonucleic acid (mRNA). Furthermore, the amount of sugar chains with an outer fucose residue, containing LewisX-BA-2, correlated well with the expression of fusocyltransferase IX mRNA. These findings add to our understanding of the molecular mechanisms responsible for the regulation of *N*-glycan biosynthesis in the cerebral cortex.**

*Key words:* cDNA macroarray/two-dimensional HPLC/*N*-linked sugar chain/pyridylamination/glycogene



## Introduction

*N*-glycans are essential for the folding, intracellular transport, stability, and secretion of glycoproteins (Helenius and Aebi, 2001). *N*-linked oligosaccharides on cell surface glycoproteins are suggested to be involved in various cellular functions including cell–cell and cell–matrix interactions. In the developing nervous system, these molecules are thought to play important roles in a wide range of events including cell adhesion, differentiation, synaptogenesis, and myelinogenesis.

Glycosylation of glycoproteins comprises a cascade of steps requiring both glycosidases and glycosyltransferases. The process is initiated in the lumen of the endoplasmic reticulum concomitant with protein translation and translocation (Geetha-Habib et al. 1988; Jenkins et al. 1996; Kornfeld and Kornfeld, 1985). The initial glycosylation event, known as *N*-linked core glycosylation, involves the transfer of a Glc3Man9GlcNAc2 unit to an acceptor asparagine residue in the tripeptide sequon Asn-Xaa-Ser/Thr and is catalyzed by the enzyme oligosaccharyl transferase (Kornfeld and Kornfeld, 1985; Geetha-Habib et al. 1988; Jenkins et al. 1996). In the *cis*-Golgi network, the initial mannose-rich core chains are trimmed by mannosidases I and II. In the *medial* and *trans*-Golgi, formation of complex type glycans ensues and is subsequently terminated by the addition of sialic acid in the *trans*-Golgi network (Kornfeld and Kornfeld, 1985; Geetha-Habib et al. 1988; Spiro and Spiro, 1991; Orlean 1992; Jenkins et al. 1996). In the past decade, a number of glycosidases and glycosyltransferases have been purified and characterized. The results support tissue-specific distribution of many kinds of glycosidases and glycosyltransferases.

More than 140 glycosyltransferase genes have been cloned (Amado et al. 1999; Herscovics, 1999; De Vries et al. 2001; Taniguchi et al. 2002; Ten Hagen et al. 2003; Harduin-Lepers et al. 2005). The data reveal families of homologous glycosyltransferases with similar catalytic activities. Thus, *N*-glycosylation pathways appear to be catalyzed by several related glycosyltransferases that may show slight differences in properties and substrate specificities. The expression levels of these enzymes are cell type or tissue specific and appear to be strictly regulated during the growth and differentiation of cells and during the tissue development. For example, α2,8-sialyltransferase V (ST8sia V) is predominantly expressed in the adult brain (Kono et al. 1996), whereas α2,8-sialyltransferase II (ST8sia II) is more highly expressed in the early stages of the development (Yoshida et al. 1995).

*These authors contributed equally to this work.
[1]To whom correspondence should be addressed; Tel: +81-564-595245; Fax: +81-564-595247; e-mail: ikenaka@nips.ac.jp

 

Thus far, no one has conducted a complete expression analysis of the full complement of "glyco-genes" during brain development. ("Glyco-genes" are those genes involved in sugar chain biosynthesis and catabolism.) Clearly, it is important to understand how glyco-gene expression is regulated during developmental changes in the brain to understand how the content of the sugar chains is regulated. For this purpose, cDNA microarray seemed to be appropriate, but it turned out that the expression levels of most of the glyco-genes were too low to be detected fluorometrically (data not shown) and glycogene-chip v1 (Comelli et al. 2006). Thus, we developed a glyco-gene macroarray system in which most of the glyco-gene cDNAs were spotted onto a nylon membrane and their expression detected by autoradiography. We also analyzed the relative amounts of *N*-linked sugar chains using two-dimensional high-performance liquid chromatography (2D-HPLC). The data were combined to precisely analyze how *N*-linked glycosylation was regulated in the brain.

## Results

### *Molecular cloning of glycosidase and glycosyltransferase genes*

As the first step to develop a cDNA macroarray system, sequence informations for glycosidase and glycosyltransferase genes were obtained from GenBank. More than 140 genes have been cloned from several species: 127 genes from the mouse, 79 genes from the rat, and 134 genes from the human. We synthesized a pair of primers around the translational start and stop codons for each gene and performed polymerase chain reactions (PCRs). As a result, we obtained DNA fragments from a total of 145 genes, which were subcloned into vector plasmids. DNA sequences were determined. DNA fragments that were cloned based on the mouse sequences were identical to the sequences reported, whereas the DNA fragments that were cloned based on the rat or human genes showed 80–90% homology to the reported ones. For example, the DNA fragments for the β1,4-galactosyltransferase VII gene showed 87.8% homology to the original human gene. We tentatively considered the resultant DNA fragments as homologs to the reported rat or human genes, because the sequences showed less homology to any other gene in the subfamily to which the original gene belonged. However, it is still possible that the fragments represent a new member of the family of glycosidase or glycosyltransferase genes. It should also be noted that the isolated rat and human DNA fragments cloned from published sequences may contain some of those original sequences (primers), although those sequences were considered to have few effects on results obtained in this study.

### *Gene expression analysis of glycosidases and glycosyltransferase by cDNA macroarray*

To determine the utility of our in-house cDNA macroarray system, a set of 145 cDNA clones were spotted onto nylon membranes using robotic printing and used to identify differentially expressed genes in a 12-week postnatal mouse brain compared with age-matched kidney and liver, and embryonic (E) 12-day fetal brain. Several housekeeping genes, β-actin, glyceraldehyde-3-phosphate dehydrogenase (GAPDH), ubiquitin B, and ribosomal protein S29 were also printed on the same array to serve as internal controls, and pZErO2 vector and λ DNA acted as negative controls. An example of one such hybridization is shown in Figure 1. The area delimited by the black line in Figure 1A shows ten 2-fold dilution steps for GAPDH. The expression level of each gene was determined by comparing the intensities of the spots with those of the dilution series. An exponential 2-fold decrease in the dilution series was obtained from expression values of 8–1. Expression values of 9 and 10 did not increase by 2-fold, suggesting that they were saturated. Although image analysis data could be obtained from an expression value of 0.1, a more reliable reading was obtained at a value of 0.5 and thus, the detection limit was defined as 0.5. cDNA macroarray data demonstrated that the gene expression patterns of glycosidases and glycosyltransferases were quite different between the two stages of brain development and among tissues (Figure 1A–D).

### *Analysis of tissue distributions by reverse transcriptase-polymerase chain reaction*

To confirm the results of our macroarray, six genes whose tissue distribution had been reported (Kono et al. 1996; Kudo et al. 1998) were selected. cDNA macroarray data demonstrated that *N*-acetylglucosaminyltransferase III (GnT III) and fucosyltransferase IX (FuT IX) were expressed in the adult kidney, E12, and adult brains. Golgi-mannosidase IB (MIB) was widely expressed among all the mouse tissues examined. Expression of the ST8sia V gene in the adult was restricted to the brain. β1,3-Galactosyltransferase I (β1,3GT1) was expressed at higher levels in the adult liver and brain than in the fetal brain. Fucosyltransferase VIII (FuT VIII) was expressed at high levels in the E12, adult brains, and kidney, but at low levels in the postnatal 12-week liver. The expression levels of these six genes were also determined by reverse transcriptase-polymerase chain reaction (RT-PCR) to confirm the differential expression in mouse tissues. The results obtained using RT-PCR were consistent with the data obtained by the macroarray system (Figure 2) and were in good agreement with the previously published data (Kono et al. 1996; Kudo et al. 1998). These results demonstrate the reliability of the cDNA macroarray system for the analysis of glyco-gene expression.

### *Gene expression analysis of glycosidases and glycosyltransferases in the mouse cerebral cortex during development*

To analyze the level at which glyco-genes were expressed during development, mRNA preparations were isolated from the cerebral cortex of E12 and E16 day fetal, and 0-day, 7-day, and 12-week postnatal mice. Isolates were subsequently analyzed on the cDNA macroarray system. The expression level of each glyco-gene in the cerebral cortex was calculated according to the intensities of the GAPDH dilution series (Figure 1A). Results are summarized in Table I.

From the array data, we found that most of the genes were expressed at very low or undetectable levels in the mouse cerebral cortex. The housekeeping genes showed expression values of 6–10 throughout development. Only the level of

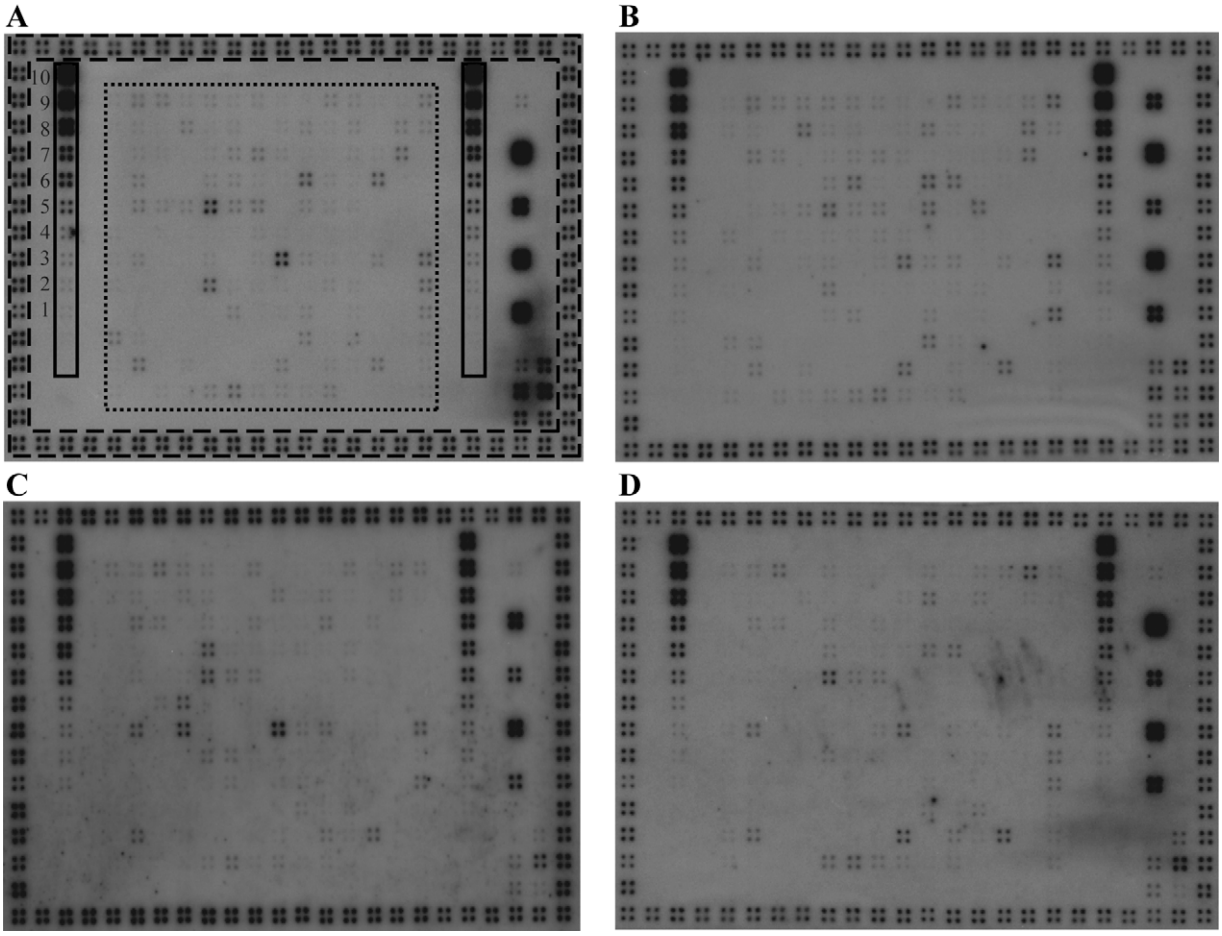


**Fig. 1.** Representative results of the cDNA macroarray. Each membrane contains quadruplicate spots (cDNA fragments) representing 145 genes implicated in the biosynthesis of sugar chains. mRNA from four mouse tissue samples, 12-day embryonic brain, 12-week postnatal brain, kidney, and liver, were extracted and then used to synthesize cDNA probes labeled with $^{32}$P-dCTP. Each probe was hybridized to a cDNA expression macroarray and images were obtained by exposing the arrays to an imaging plate. For semi-quantitative analysis, the same arrays were exposed to imaging plates to measure the radioactivity with a BAS 1800II imaging analyzer. The spots on the perimeter of the filter (within the black dash lines) are GAPDH for identification of the spot position. The boxed area delimited by the black dot lines shows the glyco-gene spotted area. The boxed area delimited by the black lines shows the dilution series of GAPDH consisting of 10 steps, each corresponding to a 2-fold dilution. (**A**) Embryonic 12-day brain, (**B**) postnatal 12-week brain, (**C**) kidney, and (**D**) liver.

α1,4-GT gene expression was comparable with those of housekeeping genes. Only three genes were expressed at levels above 3 at some point of development: O-GlcNAcase, O-GlcNAc transferase, and ST6GalNAc VI. Since we set a detection limit at 0.5, values over 0.5 have been highlighted in Table I. Those genes that failed to increase above a level of 0.5 were excluded from further analysis. However, some genes may have surpassed an expression value of 0.5 in minor cell populations in the brain. The brain consists of many types of cells and during development, there are marked changes in cell composition. However, this cDNA macroarray system was not designed to reliably detect gene expression specific to minor cell populations. Thus, analysis of glyco-gene expression was restricted to major cell populations.

Within the limits of detection, the expression levels of glyco-genes did not change markedly during development: most genes changed less than 4-fold. Nevertheless, developmental changes in gene expression were observed. For example, the levels of hexosaminidase B mRNA and ST8sia V mRNA were detected in the brain throughout development, their levels being highest in the adult cortex. In contrast, mRNA of ST8sia II was first detected in E12 fetal cortex. ST8sia II mRNA reached its maximum in the P0 cortex, after which it decreased to an almost undetectable level by 12 weeks after birth. Thus, glyco-gene expression is developmentally regulated in the brain, but does not change drastically.

### *Developmental changes in the content of N-linked sugar chains in the mouse cerebral cortex*

To investigate the correlation between glyco-gene expression and the content of *N*-linked oligosaccharides during development, we analyzed major *N*-linked sugar chains expressed in the mouse cerebral cortex at different stages during development. To simplify and enhance the analysis of sugar chain backbone synthesis and its regulation, samples were treated with neuraminidase to remove sialic acid moieties from the sugar chains. We previously found that the expression of asialo *N*-linked sugar chains is strictly regulated in the mouse cerebral cortex resulting in few differences among individuals (Fujimoto et al. 1999). Thus, cerebral cortices of 2–30 mice

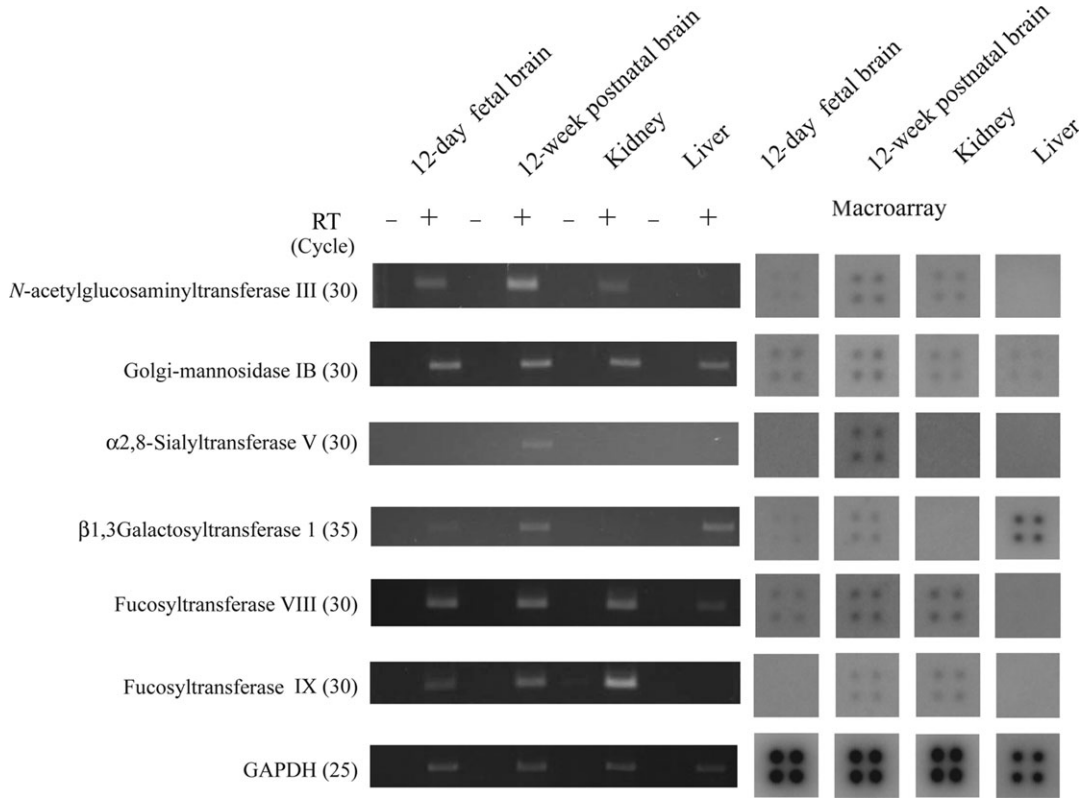


**Fig. 2.** Expression profiles of six selected genes. Gene expression was analyzed by RT-PCR using mRNAs from four mouse tissues (12-day embryonic brain, 12-week adult brain, liver, and kidney) and compared with the results obtained by cDNA macroarray. RT − or + indicate whether or not reverse transcriptase was included in the reaction mixture. The results obtained by the two methods correlated well with each other.

were pooled, homogenized together, and the sugar chain levels in only one preparation per point were analyzed. Reversed-phase HPLC resolved more than 40 peaks of pyridylamino (PA)-sugar chains from the mouse cerebral cortex. The structure of each PA-sugar chain was estimated by 2D-HPLC mapping and was confirmed by coinjection with standard PA-sugar chains. We also determined the structure of sugar chains whose standard samples were not available by enzyme digestion and mass spectrometry (Fujimoto et al., in preparation). We thus identified about 70% of the total *N*-linked sugar chains expressed in the mouse cerebral cortex. The major *N*-linked sugar chains expressed in the mouse cerebral cortex and their amounts are shown in Table III. The abbreviations and structures are given in Table II.

Since five of the identified *N*-linked sugar chains (M4B, A0G0, A0G0F, A1(6)G0F, and BA-1) are not produced by regular biosynthetic pathways, their presence might have indicated degradation during isolation. Specifically, since acetone precipitates were prepared from homogenized cerebral cortices, we were concerned about possible contamination by sugar chains degraded in the lysosome. To determine whether these sugar chains are truly present in the cell membrane, we highly purified myelin membranes by several cycles of centrifugation (Menon et al. 2003) and analyzed the resultant sugar chains. All of the sugar chains were found at comparable levels in the myelin membranes (data not shown), indicating that a major portion of these sugar chains were not degradation products.

Sugar chains were grouped into high-mannose type, hybrid type, and complex type and their developmental changes are shown in Table III. High-mannose-type sugar chains are the most abundant sugar chains among the three types and their levels were relatively constant throughout the development.

In the high-mannose series, the expression level of M5A was initially lower (E12) than those of M9A, M8A, and M6B. However, at later times, the levels of M9A, M8A, and M6B gradually decreased in the cerebral cortex, whereas M5A showed a remarkable increase, reaching a level several times higher than those of other high-mannose-type sugar chains by 12W (Table III).

One of the characteristic features of complex-type sugar chains in the brain is the abundant expression of sugar chains with bisecting GlcNAc and/or core fucose (Table III). Their levels increased only slightly during the development (Table III). On the other hand, the level of sugar chains containing α1,3-outer fucose, forming Lewis X structure, increased 2-fold during the development (Table III). We never found Sialyl-Lewis X structure in the brain (data not shown).

BA-1 and BA-2 are examples of sugar chains containing both bisecting GlcNAc and core fucose (Table III), both of which are predominantly expressed in the brain (Shimizu et al. 1993). At E12, β1,4-galactosylated BA-2 sugar chains are abundant, but the level of these sugar chains (Ga + Gb-BA-2, G2-BA-2; Table III) drops drastically up to E16, and continues to gradually decrease until adulthood (Table III).

**Table I.** Expression profile of glyco-gene (E12-, E16-, P0, P7, and 12W adult cerebral cortex)

| Glyco-gene | Accession number | E12 | E16 | P0 | P7 | 12W |
|---|---|---|---|---|---|---|
| 1 Glucosidase I | NM_020619 | **0.8 ± 0.0** | **1.1 ± 0.3** | **1.2 ± 0.4** | **1.4 ± 0.3** | **0.7 ± 0.3** |
| 2 Glucosidase II | NM_008060 | **1.1 ± 0.1** | **1.2 ± 0.2** | **1.5 ± 0.4** | **0.9 ± 0.2** | **0.6 ± 0.3** |
| 3 Acid-glucosidase α | NM_008064 | 0.1 ± 0.2 | **0.5 ± 0.4** | **0.6 ± 0.4** | **0.7 ± 0.2** | **0.8 ± 0.2** |
| 4 Acid-glucosidase β | NM_008064 | 0.1 ± 0.2 | **0.5 ± 0.2** | **0.5 ± 0.5** | **0.7 ± 0.2** | 0.3 ± 0.2 |
| 5 ER α1,2-mannosidase | XM_130073 | 0.4 ± 0.3 | **0.8 ± 0.2** | **0.8 ± 0.4** | **0.6 ± 0.1** | 0.2 ± 0.2 |
| 6 End-Mannosidase | NM_172865 | 0.0 ± 0.0 | 0.0 ± 0.1 | 0.1 ± 0.1 | 0.3 ± 0.3 | 0.0 ± 0.0 |
| 7 Golgi-mannaosidase IA | NM_008548 | 0.0 ± 0.0 | 0.0 ± 0.0 | 0.2 ± 0.2 | 0.1 ± 0.1 | 0.0 ± 0.0 |
| 8 Golgi-mannaosidase IB | NM_010763 | **0.7 ± 0.2** | **1.1 ± 0.0** | **1.1 ± 0.3** | **1.7 ± 0.3** | **1.3 ± 0.3** |
| 9 Golgi-mannaosidase IC | NM_207237 | 0.0 ± 0.0 | 0.1 ± 0.1 | 0.2 ± 0.2 | 0.3 ± 0.2 | 0.1 ± 0.1 |
| 10 Mannosidase II | NM_008549 | **0.8 ± 0.2** | **1.4 ± 0.3** | **1.8 ± 0.2** | **2.0 ± 0.3** | **1.6 ± 0.4** |
| 11 Mannosidase IIx | NM_172903 | 0.0 ± 0.0 | 0.2 ± 0.1 | 0.3 ± 0.2 | 0.4 ± 0.2 | 0.0 ± 0.0 |
| 12 Putative-mannosidase 3 | AK079296 | 0.2 ± 0.2 | **0.8 ± 0.2** | **0.9 ± 0.3** | **0.8 ± 0.1** | 0.4 ± 0.1 |
| 13 Lysosomal α-mannosidase | NM_010764 | 0.2 ± 0.2 | **0.8 ± 0.0** | **0.7 ± 0.3** | **1.0 ± 0.1** | 0.3 ± 0.2 |
| 14 Lysosomal β-mannosidase | NM_027288 | 0.0 ± 0.0 | 0.2 ± 0.1 | 0.2 ± 0.1 | 0.2 ± 0.0 | 0.0 ± 0.0 |
| 15 α-mannosidase (MAN2B2) | AB006458 | 0.2 ± 0.2 | **0.5 ± 0.1** | **0.6 ± 0.1** | **0.8 ± 0.1** | **0.5 ± 0.2** |
| 16 α-mannosidase (6A8) | AF044414 | 0.1 ± 0.2 | 0.3 ± 0.1 | 0.3 ± 0.3 | 0.1 ± 0.2 | 0.2 ± 0.1 |
| 17 Cytosolic α-D-mannosidase | NM_028636 | 0.1 ± 0.1 | 0.4 ± 0.2 | **0.5 ± 0.2** | 0.4 ± 0.3 | 0.3 ± 0.1 |
| 18 GnT I | NM_010794 | **0.6 ± 0.1** | 0.4 ± 0.2 | **0.9 ± 0.1** | **0.7 ± 0.4** | **0.6 ± 0.1** |
| 19 GnT 1.2 | AB053220 | **0.5 ± 0.2** | **0.5 ± 0.2** | **1.0 ± 0.3** | **1.0 ± 0.3** | **0.5 ± 0.1** |
| 20 GnT II | NM_146035 | **0.7 ± 0.1** | **0.7 ± 0.4** | **1.0 ± 0.5** | **0.6 ± 0.4** | 0.3 ± 0.0 |
| 21 GnT III | NM_010795 | **0.6 ± 0.1** | **0.8 ± 0.2** | **1.3 ± 0.3** | **1.3 ± 0.3** | **1.2 ± 0.2** |
| 22 GnT IV A | NM_173870 | 0.3 ± 0.2 | 0.4 ± 0.0 | **0.6 ± 0.0** | **0.8 ± 0.5** | **0.5 ± 0.3** |
| 23 GnT IV B | NM_145926 | **0.8 ± 0.0** | **1.2 ± 0.1** | **2.0 ± 0.3** | **2.1 ± 0.4** | **0.7 ± 0.1** |
| 24 GnT IV H | NM_026243 | 0.1 ± 0.1 | 0.0 ± 0.0 | 0.0 ± 0.0 | 0.2 ± 0.4 | 0.1 ± 0.2 |
| 25 GnT V | AF474154 | **0.5 ± 0.2** | **0.8 ± 0.1** | **1.1 ± 0.2** | **1.0 ± 0.6** | **1.1 ± 0.1** |
| 26 GnT IX | AB119127 | 1.1 ± 0.0 | **1.8 ± 0.1** | **2.5 ± 0.4** | **2.1 ± 0.7** | **1.2 ± 0.1** |
| 27 β1,3GnT 1 | NM_016888 | 0.1 ± 0.1 | 0.2 ± 0.2 | 0.1 ± 0.1 | **0.5 ± 0.8** | 0.4 ± 0.2 |
| 28 β1,3GnT 3 | AY037785 | 0.0 ± 0.1 | 0.0 ± 0.0 | 0.1 ± 0.1 | 0.2 ± 0.4 | 0.0 ± 0.1 |
| 29 β1,3GnT 4 | AY037786 | 0.1 ± 0.2 | 0.1 ± 0.1 | 0.3 ± 0.2 | **0.5 ± 0.5** | 0.3 ± 0.3 |
| 30 β1,3GnT 5 (Lc3 synthase) | AY029203 | 0.4 ± 0.1 | **0.6 ± 0.2** | **0.8 ± 0.3** | **0.5 ± 0.7** | 0.2 ± 0.2 |
| 31 β1,3GnT 7 | AF502429 | 0.1 ± 0.1 | 0.2 ± 0.2 | 0.2 ± 0.2 | 0.3 ± 0.4 | 0.2 ± 0.3 |
| 32 Manic fringe | AF015769 | **0.8 ± 0.1** | 0.2 ± 0.1 | **0.6 ± 0.3** | 0.0 ± 0.0 | 0.1 ± 0.1 |
| 33 Lunatic fringe | AF015768 | 0.2 ± 0.1 | 0.1 ± 0.2 | 0.3 ± 0.2 | 0.2 ± 0.2 | 0.2 ± 0.2 |
| 34 Radical fringe | AF015770 | 0.3 ± 0.1 | **0.7 ± 0.2** | **0.9 ± 0.2** | **1.2 ± 0.1** | **0.6 ± 0.3** |
| 35 LARGE | AJ006278 | 0.2 ± 0.2 | **0.6 ± 0.4** | **1.1 ± 0.5** | **1.4 ± 0.0** | **0.8 ± 0.4** |
| 36 i-β1,3GnT | NM_175383 | 0.0 ± 0.0 | 0.0 ± 0.0 | 0.3 ± 0.2 | 0.3 ± 0.3 | 0.1 ± 0.2 |
| 37 I GnTA | AB037597 | 0.1 ± 0.1 | 0.0 ± 0.0 | **0.5 ± 0.4** | **1.2 ± 0.7** | 0.3 ± 0.2 |
| 38 I GnTB | AB037596 | 0.0 ± 0.1 | 0.1 ± 0.2 | **0.8 ± 0.3** | **1.3 ± 0.4** | **0.5 ± 0.2** |
| 39 O-GlcNAc Transferase | NM_139144 | **2.2 ± 0.1** | **4.4 ± 0.1** | **3.8 ± 0.3** | **2.9 ± 0.4** | **2.9 ± 0.2** |
| 40 C2GnT1 | NM_010265 | 0.0 ± 0.0 | 0.1 ± 0.1 | 0.2 ± 0.1 | 0.1 ± 0.1 | 0.0 ± 0.1 |
| 41 C2GnT2 | NM_028087 | 0.0 ± 0.0 | 0.0 ± 0.0 | **0.5 ± 0.2** | 0.2 ± 0.2 | 0.3 ± 0.2 |
| 42 C2GnT3 | XM_138797 | 0.1 ± 0.2 | 0.4 ± 0.2 | **0.7 ± 0.1** | 0.4 ± 0.4 | **0.7 ± 0.4** |
| 43 Fucosyltransferase I | NM_008051 | 0.0 ± 0.0 | 0.0 ± 0.0 | 0.4 ± 0.4 | 0.0 ± 0.0 | 0.1 ± 0.1 |
| 44 Fucosyltransferase II | NM_018876 | 0.0 ± 0.0 | 0.0 ± 0.1 | 0.3 ± 0.4 | 0.0 ± 0.0 | 0.1 ± 0.1 |
| 45 Fucosyltransferase IV | NM_010242 | 0.0 ± 0.0 | 0.1 ± 0.2 | 0.2 ± 0.1 | 0.1 ± 0.1 | 0.2 ± 0.2 |
| 46 Fucosyltransferase VII | NM_013524 | 0.0 ± 0.0 | 0.1 ± 0.1 | 0.4 ± 0.4 | 0.1 ± 0.1 | 0.2 ± 0.1 |
| 47 Fucosyltransferase VIII | NM_016893 | 0.0 ± 0.1 | 0.3 ± 0.1 | **0.6 ± 0.3** | **0.7 ± 0.3** | 0.2 ± 0.1 |

*Continued*

**Table I.** *Continued*

| Glyco-gene | Accession number | E12 | E16 | P0 | P7 | 12W |
|---|---|---|---|---|---|---|
| 48 Fucosyltransferase IX | NM_010243 | 0.1 ± 0.1 | **0.7 ± 0.1** | **1.1 ± 0.6** | **1.1 ± 0.4** | **0.8 ± 0.2** |
| 49 Fucosyltransferase X | NM_134161 | 0.0 ± 0.0 | 0.0 ± 0.0 | 0.2 ± 0.1 | 0.0 ± 0.0 | 0.0 ± 0.0 |
| 50 Fusocyltransferase XI | XM_203633 | 0.1 ± 0.1 | 0.3 ± 0.1 | **0.7 ± 0.3** | **0.5 ± 0.5** | 0.1 ± 0.2 |
| 51 Fucosyltransferase Sec 1 | NM_019934 | 0.0 ± 0.0 | 0.2 ± 0.2 | 0.3 ± 0.3 | 0.1 ± 0.1 | 0.1 ± 0.1 |
| 52 O-Fucosyltransferase 1 | NM_080463 | **0.5 ± 0.2** | **0.6 ± 0.1** | **0.8 ± 0.3** | 0.4 ± 0.4 | 0.1 ± 0.1 |
| 53 O-Fucosyltransferase 2 | NM_030262 | 0.0 ± 0.0 | 0.0 ± 0.0 | 0.2 ± 0.2 | 0.1 ± 0.1 | 0.0 ± 0.0 |
| 54 Hexosaminidase A | NM_010421 | 0.4 ± 0.1 | **0.7 ± 0.2** | **0.9 ± 0.5** | **0.8 ± 0.3** | **0.7 ± 0.4** |
| 55 Hexosaminidase B | NM_010422 | 0.2 ± 0.2 | **1.0 ± 0.1** | **1.0 ± 0.4** | **1.5 ± 0.2** | **1.7 ± 0.4** |
| 56 β1,3GT I | AF029790 | 0.2 ± 0.2 | 0.4 ± 0.1 | **0.5 ± 0.2** | **0.6 ± 0.1** | 0.3 ± 0.1 |
| 57 β1,3GT II | NM_020025 | 0.1 ± 0.2 | **0.6 ± 0.3** | **0.5 ± 0.3** | **0.7 ± 0.2** | **0.5 ± 0.1** |
| 58 β1,3GT III | AF029792 | 0.2 ± 0.2 | **0.5 ± 0.1** | **0.7 ± 0.5** | **0.9 ± 0.3** | 0.3 ± 0.1 |
| 59 β1,3GT IIV | AF082504 | 0.2 ± 0.0 | 0.0 ± 0.1 | 0.3 ± 0.4 | 0.1 ± 0.1 | 0.0 ± 0.0 |
| 60 β1,3GT V | AF254738 | 0.1 ± 0.1 | 0.1 ± 0.1 | 0.2 ± 0.2 | 0.2 ± 0.3 | 0.3 ± 0.3 |
| 61 β1,3GT VI | NM_080445 | 0.2 ± 0.1 | 0.1 ± 0.1 | 0.1 ± 0.2 | 0.0 ± 0.0 | 0.2 ± 0.4 |
| 62 β1,3GT VIII | NM_052993 | 0.1 ± 0.1 | 0.1 ± 0.1 | 0.2 ± 0.4 | 0.0 ± 0.0 | 0.1 ± 0.2 |
| 63 β1,4GT I | NM_022305 | 0.3 ± 0.1 | 0.1 ± 0.1 | 0.3 ± 0.0 | 0.1 ± 0.2 | 0.2 ± 0.1 |
| 64 β1,4GT II | AF142670 | 0.2 ± 0.1 | 0.4 ± 0.2 | **0.7 ± 0.2** | **0.8 ± 0.2** | 0.3 ± 0.3 |
| 65 β1,4GT III | BC013619 | **0.5 ± 0.0** | **0.7 ± 0.1** | **0.8 ± 0.3** | 0.3 ± 0.2 | 0.4 ± 0.1 |
| 66 β1,4GT IV | AF142672 | 0.2 ± 0.2 | 0.2 ± 0.2 | 0.3 ± 0.3 | 0.0 ± 0.0 | 0.2 ± 0.2 |
| 67 β1,4GT V | NM_019835 | 0.3 ± 0.1 | **0.5 ± 0.4** | **0.7 ± 0.1** | **0.8 ± 0.2** | **0.5 ± 0.3** |
| 68 β1,4GT VI | NM_019737 | 0.2 ± 0.1 | **0.5 ± 0.3** | **1.1 ± 0.3** | **1.7 ± 0.2** | **1.1 ± 0.2** |
| 69 β1,4GT VII | NM_146045 | 0.0 ± 0.0 | 0.1 ± 0.2 | 0.3 ± 0.5 | 0.0 ± 0.0 | 0.3 ± 0.2 |
| 70 α1,3GT | NM_010283 | 0.1 ± 0.2 | 0.1 ± 0.2 | 0.4 ± 0.5 | 0.1 ± 0.1 | **0.5 ± 0.4** |
| 71 α1,4GT | AJ245581 | **6.2 ± 0.3** | **9.4 ± 0.8** | **8.0 ± 1.9** | **6.5 ± 0.7** | **7.0 ± 0.7** |
| 72 ST3 Gal I | NM_009177 | 0.3 ± 0.2 | 0.2 ± 0.1 | 0.2 ± 0.1 | 0.3 ± 0.3 | 0.0 ± 0.1 |
| 73 ST3Gal II | NM_009179 | **0.6 ± 0.0** | **0.6 ± 0.3** | **1.2 ± 0.6** | **1.1 ± 0.1** | **0.8 ± 0.2** |
| 74 ST3Gal III | NM_009176 | 0.2 ± 0.1 | 0.2 ± 0.2 | 0.2 ± 0.3 | 0.3 ± 0.3 | 0.3 ± 0.2 |
| 75 ST3Gal IV | NM_009178 | 0.3 ± 0.0 | 0.3 ± 0.1 | 0.3 ± 0.2 | 0.2 ± 0.2 | 0.3 ± 0.1 |
| 76 ST3Gal V | NM_011375 | 0.2 ± 0.1 | 0.3 ± 0.1 | 0.4 ± 0.5 | 0.4 ± 0.2 | **0.9 ± 0.1** |
| 77 ST3Gal VI | AF119390 | 0.0 ± 0.1 | 0.1 ± 0.1 | 0.1 ± 0.2 | 0.0 ± 0.1 | 0.2 ± 0.3 |
| 78 ST6Gal I | NM_145933 | 0.4 ± 0.1 | **0.7 ± 0.3** | **0.5 ± 0.3** | 0.2 ± 0.2 | 0.2 ± 0.1 |
| 79 ST6Gal II | AB095093 | **0.5 ± 0.0** | **1.5 ± 0.2** | **2.4 ± 0.6** | **1.8 ± 0.5** | **0.9 ± 0.0** |
| 80 ST6 GalNAc I | NM_011371 | 0.1 ± 0.2 | 0.1 ± 0.1 | 0.3 ± 0.4 | 0.1 ± 0.1 | 0.3 ± 0.1 |
| 81 ST6 GalNAc II | NM_009180 | 0.1 ± 0.1 | 0.2 ± 0.2 | 0.3 ± 0.3 | 0.0 ± 0.0 | 0.2 ± 0.2 |
| 82 ST6 GalNAc III | NM_011372 | 0.1 ± 0.1 | 0.1 ± 0.1 | 0.4 ± 0.4 | 0.1 ± 0.1 | 0.1 ± 0.2 |
| 83 ST6GalNAc IV | NM_011373 | 0.1 ± 0.1 | 0.2 ± 0.1 | 0.3 ± 0.3 | 0.3 ± 0.2 | 0.3 ± 0.1 |
| 84 ST6GalNAc V | NM_012028 | **2.5 ± 0.1** | **4.2 ± 0.1** | **4.2 ± 0.4** | **4.1 ± 0.4** | **3.4 ± 0.2** |
| 85 ST6GalNAc VI | NM_016973 | 0.2 ± 0.2 | 0.3 ± 0.2 | **0.7 ± 0.4** | **1.0 ± 0.2** | **1.2 ± 0.1** |
| 86 ST8Sia I | NM_011374 | 0.1 ± 0.1 | 0.2 ± 0.2 | 0.4 ± 0.5 | 0.0 ± 0.0 | 0.4 ± 0.2 |
| 87 ST8Sia II | NM_009181 | **0.6 ± 0.1** | **1.9 ± 0.2** | **2.8 ± 0.4** | **1.2 ± 0.4** | 0.2 ± 0.0 |
| 88 ST8Sia III | NM_009182 | 0.0 ± 0.0 | **0.5 ± 0.2** | **1.3 ± 0.3** | **1.3 ± 0.2** | **0.9 ± 0.1** |
| 89 ST8Sia IV | NM_009183 | 0.0 ± 0.1 | 0.4 ± 0.2 | **0.9 ± 0.5** | 0.1 ± 0.1 | 0.3 ± 0.2 |
| 90 ST8Sia V | NM_013666 | 0.0 ± 0.0 | 0.1 ± 0.2 | 0.4 ± 0.3 | **0.6 ± 0.3** | **1.0 ± 0.1** |
| 91 ST8Sia VI | NM_145838 | 0.1 ± 0.1 | 0.1 ± 0.1 | 0.2 ± 0.0 | 0.2 ± 0.1 | 0.3 ± 0.2 |
| 92 O-Mannosyltransferase 1 | NM_145145 | 0.0 ± 0.1 | 0.2 ± 0.2 | **0.6 ± 0.3** | 0.3 ± 0.3 | 0.1 ± 0.1 |
| 93 O-Mannosyltransferase 2 | AY090482 | 0.0 ± 0.0 | 0.2 ± 0.1 | 0.3 ± 0.3 | 0.3 ± 0.3 | 0.1 ± 0.2 |
| 94 *N*-sulfoglucosamine sulfohydrolase | NM_018822 | 0.1 ± 0.2 | 0.3 ± 0.1 | **0.6 ± 0.2** | 0.4 ± 0.2 | 0.1 ± 0.1 |

*Continued*

**Table I.** *Continued*

| Glyco-gene | Accession number | E12 | E16 | P0 | P7 | 12W |
|---|---|---|---|---|---|---|
| 95 Fukutin | NM_139309 | 0.1 ± 0.1 | 0.4 ± 0.1 | 0.2 ± 0.1 | 0.2 ± 0.3 | 0.2 ± 0.2 |
| 96 Fukutin related protein | NM_173430 | 0.0 ± 0.0 | 0.2 ± 0.1 | 0.1 ± 0.1 | 0.0 ± 0.0 | 0.1 ± 0.1 |
| 97 α-L-Fucosidase | NM_024243 | 0.2 ± 0.3 | **0.5 ± 0.3** | **0.6 ± 0.6** | **0.7 ± 0.1** | 0.3 ± 0.3 |
| 98 Neuraminidase 1 | NM_010893 | 0.1 ± 0.2 | **0.6 ± 0.5** | **0.7 ± 0.3** | **0.9 ± 0.4** | **0.7 ± 0.2** |
| 99 Neuraminidase 2 | NM_015750 | 0.1 ± 0.1 | 0.2 ± 0.1 | 0.2 ± 0.1 | 0.1 ± 0.1 | 0.2 ± 0.2 |
| 100 Neuraminidase 3 | NM_016720 | 0.1 ± 0.1 | 0.3 ± 0.0 | **0.6 ± 0.2** | 0.3 ± 0.1 | 0.1 ± 0.1 |
| 101 α-L-idulonidase | L34111 | 0.1 ± 0.2 | **0.6 ± 0.3** | **0.6 ± 0.2** | **0.5 ± 0.3** | 0.1 ± 0.2 |
| 102 EXT1 | U78539 | **0.9 ± 0.1** | **1.1 ± 0.3** | **1.9 ± 0.4** | **1.6 ± 0.2** | **1.0 ± 0.2** |
| 103 EXT2 | U67837 | **0.5 ± 0.1** | 0.4 ± 0.2 | **1.0 ± 0.7** | **0.7 ± 0.2** | 0.3 ± 0.2 |
| 104 Exostoses (multiple)-like 1 | NM_019578 | 0.1 ± 0.1 | 0.3 ± 0.3 | **0.6 ± 0.2** | **0.7 ± 0.2** | **1.3 ± 0.2** |
| 105 Exostoses (multiple)-like 2 | NM_021388 | 0.0 ± 0.0 | 0.1 ± 0.1 | 0.1 ± 0.1 | 0.2 ± 0.3 | 0.1 ± 0.2 |
| 106 Exostoses (multiple)-like 3 | NM_018788 | 0.0 ± 0.0 | 0.1 ± 0.1 | **0.5 ± 0.4** | 0.4 ± 0.5 | 0.3 ± 0.2 |
| 107 Xylosyltransferase 1 | AJ291750 | 0.2 ± 0.1 | 0.1 ± 0.1 | **0.7 ± 0.2** | **0.5 ± 0.4** | 0.3 ± 0.2 |
| 108 Xylosyltransferase 2 | AJ291751 | 0.2 ± 0.1 | 0.1 ± 0.2 | 0.4 ± 0.3 | 0.4 ± 0.4 | 0.2 ± 0.1 |
| 109 GlcNAc-P-Glycosidase | NM_016256 | 0.1 ± 0.1 | 0.1 ± 0.1 | 0.3 ± 0.2 | 0.4 ± 0.3 | 0.1 ± 0.0 |
| 110 Polypeptide GalNAc T1 | NM_013814 | **0.5 ± 0.1** | 0.4 ± 0.0 | **0.5 ± 0.2** | **0.7 ± 0.4** | 0.2 ± 0.1 |
| 111 Polypeptide GalNAc T2 | AF348968 | **0.8 ± 0.2** | **0.8 ± 0.1** | **1.4 ± 0.1** | **1.6 ± 0.8** | **0.6 ± 0.3** |
| 112 Polypeptide GalNAc T3 | NM_015736 | 0.0 ± 0.0 | 0.1 ± 0.1 | 0.2 ± 0.2 | 0.0 ± 0.0 | 0.0 ± 0.0 |
| 113 Polypeptide GalNAc T4 | NM_015737 | 0.0 ± 0.0 | 0.1 ± 0.2 | 0.2 ± 0.2 | 0.1 ± 0.2 | 0.0 ± 0.1 |
| 114 Polypeptide GalNAc T5 | AF049344 | 0.0 ± 0.0 | 0.0 ± 0.1 | 0.1 ± 0.2 | 0.0 ± 0.1 | 0.1 ± 0.1 |
| 115 Polypeptide GalNAc T6 | AJ133523 | 0.0 ± 0.0 | 0.1 ± 0.1 | 0.3 ± 0.1 | 0.2 ± 0.0 | 0.2 ± 0.2 |
| 116 Polypeptide GalNAc T7 | AF349573 | 0.4 ± 0.1 | 0.3 ± 0.2 | **0.5 ± 0.1** | **0.7 ± 0.5** | 0.3 ± 0.1 |
| 117 Polypeptide GalNAc T9 | AF241241 | 0.0 ± 0.0 | 0.1 ± 0.2 | 0.1 ± 0.2 | 0.0 ± 0.1 | 0.0 ± 0.0 |
| 118 Polypeptide GalNAc T13 | AB082928 | 0.1 ± 0.1 | 0.3 ± 0.1 | **0.5 ± 0.3** | **0.7 ± 0.1** | **0.9 ± 0.4** |
| 119 ABO blood group | NM_030718 | 0.0 ± 0.0 | 0.1 ± 0.2 | 0.3 ± 0.5 | 0.0 ± 0.0 | 0.0 ± 0.1 |
| 120 1,4(GM2 synthase) | NM_008080 | 0.1 ± 0.2 | **1.4 ± 0.3** | **1.9 ± 0.4** | **2.2 ± 0.2** | **1.5 ± 0.3** |
| 121 Ceramide glycosyltransferase | NM_011673 | **0.8 ± 0.1** | **1.4 ± 0.1** | **1.8 ± 0.5** | **1.9 ± 0.1** | **1.1 ± 0.1** |
| 122 α-*N*-acetylglucosaminidase | NM_013792 | 0.1 ± 0.1 | 0.2 ± 0.1 | **0.5 ± 0.6** | 0.1 ± 0.1 | 0.1 ± 0.1 |
| 123 O-GlcNAcase | NM_023799 | **2.1 ± 0.4** | **3.2 ± 0.2** | **3.8 ± 0.5** | **3.3 ± 0.3** | **2.3 ± 0.2** |
| 124 Chondroitin-6-sulfotransferase | NM_016803 | 0.2 ± 0.1 | 0.3 ± 0.0 | **1.1 ± 0.0** | 0.1 ± 0.1 | 0.3 ± 0.3 |
| 125 Galactose 6-O-sulfotransferase | AF280087 | 0.1 ± 0.1 | 0.4 ± 0.1 | **1.2 ± 0.3** | **0.9 ± 0.1** | **1.5 ± 0.5** |
| 126 Dermatan-4-sulfotransferase | NM_028117 | 0.1 ± 0.1 | 0.3 ± 0.1 | 0.4 ± 0.1 | 0.1 ± 0.1 | 0.1 ± 0.2 |
| 127 GST1 | NM_016922 | 0.0 ± 0.0 | 0.0 ± 0.0 | 0.2 ± 0.2 | 0.0 ± 0.1 | 0.0 ± 0.0 |
| 128 HS2ST1 | NM_011828 | **0.5 ± 0.1** | 0.4 ± 0.2 | **0.6 ± 0.3** | **1.1 ± 0.1** | 0.3 ± 0.3 |
| 129 HS3ST1 | NM_010474 | 0.0 ± 0.0 | 0.1 ± 0.1 | 0.3 ± 0.1 | **1.1 ± 0.3** | 0.1 ± 0.1 |
| 130 HS3ST3A | NM_006042 | 0.1 ± 0.1 | 0.1 ± 0.1 | 0.2 ± 0.2 | 0.3 ± 0.3 | 0.2 ± 0.3 |
| 131 HS3ST3B | NM_018805 | 0.0 ± 0.1 | 0.1 ± 0.1 | 0.2 ± 0.2 | 0.3 ± 0.5 | 0.1 ± 0.1 |
| 132 HS6ST1 | NM_015818 | 0.1 ± 0.1 | 0.4 ± 0.1 | **0.6 ± 0.3** | **1.0 ± 0.5** | 0.2 ± 0.1 |
| 133 HS6ST2 | NM_015819 | 0.4 ± 0.2 | **1.3 ± 0.2** | **1.7 ± 0.3** | **1.1 ± 0.4** | 0.4 ± 0.1 |
| 134 HS6ST3 | NM_015820 | 0.0 ± 0.0 | 0.2 ± 0.1 | 0.2 ± 0.2 | **0.5 ± 0.5** | 0.2 ± 0.4 |
| 135 NDST1 | AF074926 | 0.3 ± 0.2 | 0.4 ± 0.2 | **0.7 ± 0.0** | **0.7 ± 0.4** | 0.1 ± 0.1 |
| 136 NDST2 | NM_010811 | 0.1 ± 0.1 | 0.3 ± 0.3 | 0.3 ± 0.3 | 0.2 ± 0.3 | 0.0 ± 0.1 |
| 137 NDST3 | NM_031186 | 0.1 ± 0.1 | 0.4 ± 0.2 | 0.3 ± 0.3 | 0.2 ± 0.2 | 0.2 ± 0.3 |
| 138 NSDT4 | NM_022565 | 0.0 ± 0.0 | 0.4 ± 0.1 | 0.2 ± 0.1 | 0.4 ± 0.4 | 0.2 ± 0.3 |
| 139 Chondroitin GalNAcT1 | NM_172753 | 0.1 ± 0.1 | 0.0 ± 0.0 | 0.1 ± 0.2 | 0.3 ± 0.5 | 0.0 ± 0.0 |
| 140 Chondroitin sulfate GalNAcT2 | NM_030165 | 0.2 ± 0.2 | **0.7 ± 0.1** | **0.8 ± 0.2** | **0.7 ± 0.3** | 0.4 ± 0.2 |
| 141 GalNAc4ST1 | NM_175140 | 0.2 ± 0.2 | 0.4 ± 0.5 | **0.7 ± 0.3** | 0.4 ± 0.3 | 0.4 ± 0.1 |

*Continued*

**Table I.** *Continued*

| Glyco-gene | Accession number | E12 | E16 | P0 | P7 | 12W |
|---|---|---|---|---|---|---|
| 142 GalNAc4ST2 | XM_128967 | 0.0 ± 0.0 | 0.2 ± 0.4 | 0.2 ± 0.3 | 0.2 ± 0.2 | 0.1 ± 0.2 |
| 143 GalNAc4,6ST2 | NM_022935 | **0.5 ± 0.2** | **0.7 ± 0.2** | **1.0 ± 0.4** | **1.3 ± 0.1** | **0.5 ± 0.3** |
| 144 Chondrloitin 4-O-sulfotransferase 1 | AJ289133 | 0.0 ± 0.0 | 0.3 ± 0.5 | 0.2 ± 0.2 | 0.0 ± 0.0 | 0.0 ± 0.0 |
| 145 Chondroitin 4-O-sulfotransferase 2 | AJ289132 | 0.3 ± 0.1 | **0.8 ± 0.4** | **0.8 ± 0.3** | **0.6 ± 0.0** | 0.4 ± 0.2 |

Data are expressed as the means ± standard errors of the means of values obtained from the three independent experiments.
Boldface values indicate the expression level (means > 0.5).

In contrast, there are steep increases in the levels of BA-2 or β1,4-galactosylated BA-2 with outer fucose residue (LewisX-BA-2). Later in the development, there are increases in BA-1 sugar chain, which is generated from BA-2 through the action of hexosaminidase (Okamoto et al. 1999).

Another interesting feature is the presence of *N*-linked sugar chains containing Gal residues connected via β1-3 linkages, which appeared after birth (Table III).

## Discussion

### *The combination of HPLC system and cDNA macroarray system*

In this report, we combined two analytical systems, HPLC and cDNA macroarray, and successfully compared the population of *N*-linked sugar chains and glyco-gene expression levels during the course of mouse cerebral cortex development (Tables I and III). HPLC analysis is necessary for the identification of sugar chain in order to isolate and identify the isomers of *N*-glycan expressed in the tissue. For example, A2G2F and A2G′2F are isomer structure of *N*-glycan, but separated in different elution time in the reversed-phase HPLC.

Some other researchers also developed microarray system for mouse (Comelli et al. 2006) and human glyco-genes (Kemmner et al. 2003), though these systems lack some of the genes included in the present study. For example, glyco-gene chip v1 missed most of mannosidase genes, which are not covered even at the latest version of gene chip (glyco-gene v.3). In addition, the expression levels of most of the glyco-genes were too low to be detected fluorometrically; hence, redesign of the probe set was necessary (Comelli et al. 2006). Thus, we developed a glyco-gene cDNA macroarray system and their expression was detected by autoradiography.

### *Major pathway for biosynthesis of N-linked sugar chains in the cerebral cortex*

In this report, we describe the structures of those *N*-linked sugar chains exceeding 0.1% of total *N*-linked sugar chains in the cerebral cortex. From these data, we constructed a pathway for biosynthesis of major *N*-linked sugars in the brain (Figure 3). The sugar chains within parentheses were not found, but it is reasonable to assume that the pathway went through these intermediates. Expression of all the genes required for this biosynthetic model was detected through our cDNA macroarray system. Although many glyco-genes are involved in *N*-linked sugar chain biosynthesis, the major biosynthetic pathway in the brain seems to utilize a relatively small number of the genes (Table I). Other than β1,3 and β1,4 galactosyltransferases, each enzyme is expressed by a single gene in the brain.

### *Changes in high-mannose-type sugar chain levels in the cerebral cortex during development*

In the cerebral cortex at E12, there was more M9A, M8A, and M6B than M5A; however, the first three chains decreased gradually as development proceeded. In contrast, the M5A content gradually increased during the development. In fact, by 12W, M5A reached a level several times higher than those of other oligomannose-type sugar chains (Table III). These results suggest that cell surface oligomannose *N*-linked sugar chains may be particularly important, and their expression should be strictly regulated in the cerebral cortex during the development. Indeed, oligomannose *N*-linked sugar chains are present on the surface of neural cells (Schmitz et al. 1993). Furthermore, it has been suggested that oligomannose *N*-linked sugar chains may play important roles in processes such as synaptic formation (Dontenwill et al. 1985) and myelination (Kuchler et al. 1989) in the central nervous system during the development. Our results suggest that M5A may have a unique function in the brain that cannot be replaced by other high mannose-type sugar chains.

The enzyme that is mainly responsible for the generation of M5A in the *cis*-Golgi body in the cortex is MIB (Figure 3 and Table I). The MIB mRNA levels increased 2-fold from E12 to P7 (expression values of 0.7–1.7) and declined slightly in adulthood (Table I), which is consistent with the decrease in the level of the initial substrate, M8A, and the increase in the level of final product, M5A, in the *cis*-Golgi during the development. However, we have to take into consideration the vesicle transport into and out of the *cis*-Golgi body, MIB enzyme activity, and the availability of substrate sugar chains on the protein. For those reasons, it would be intriguing to change the MIB level in the cortex to determine the impact on high-mannose-type sugar chains.

### *Developmental regulation of BA-1 and BA-2 biosynthesis and their related sugar chains in the cerebral cortex*

*N*-linked sugar chains in the brain often carry bisecting GlcNAc and/or core fucose (Table II). The mRNA levels of GnT III and FuT VIII were reported to be high in the brain (Miyoshi et al. 1997). The mRNA level of GnT III was also detected in our macroarray system throughout the developmental stage (Table I). On the other hand, FuT VIII was not detected during embryonic stages even though there were abundant sugar chains with core fucose structures (Table III)

**Table II.** Abbreviations and structures of PA-sugar chains

| Abbreviations | Structure |
|---|---|
| (1) M9A | 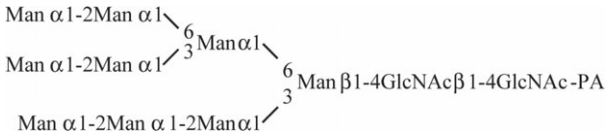 |
| (2) M8A | 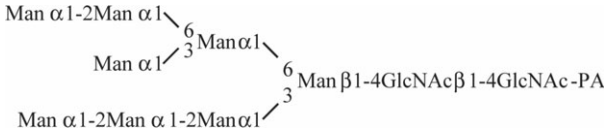 |
| (3) M7A | 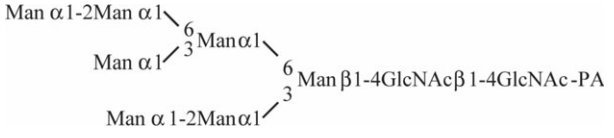 |
| (4) M7B | 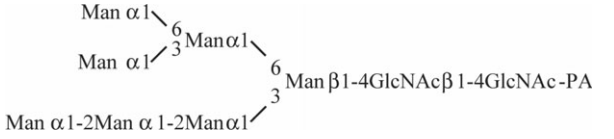 |
| (5) M6B | 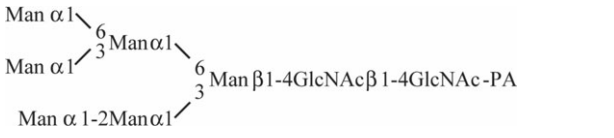 |
| (6) M5A | 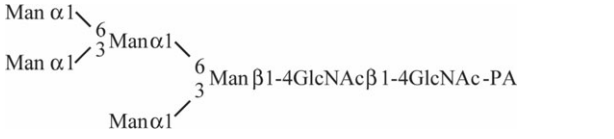 |
| (7) M4B | 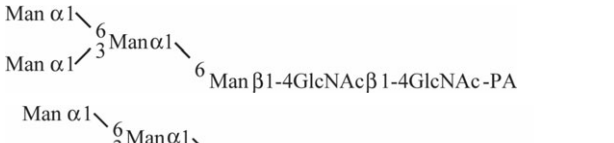 |
| (8) H5.1 | 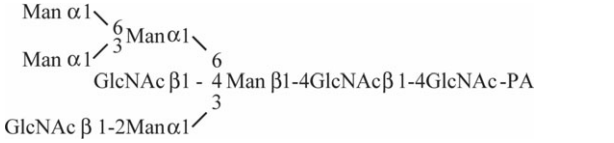 |
| (9) LewisX-H4FB | 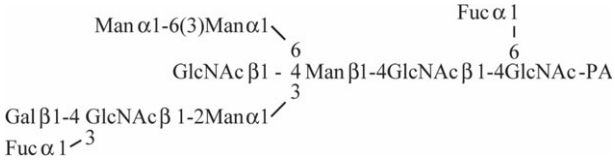 |
| (10) A0G0 | 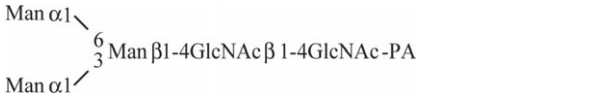 |
| (11) LewisX-H5F | 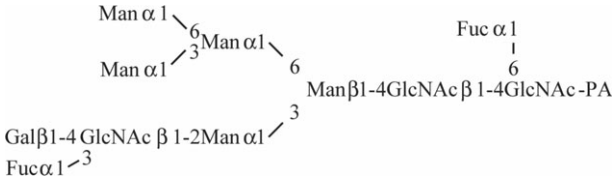 |
| (12) A0G0F | 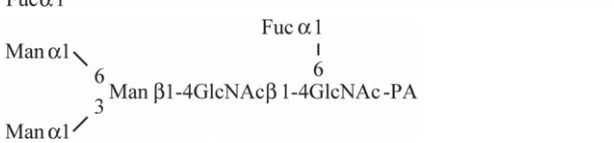 |

*Continued*

**Table II.** *Continued*

| Abbreviations | Structure |
|---|---|
| (13) A1(6)G0F | 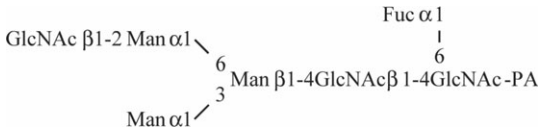 |
| (14) BA-1 | 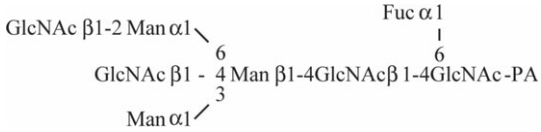 |
| (15) A2G0B | 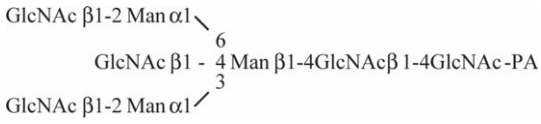 |
| (16) BA-2 | 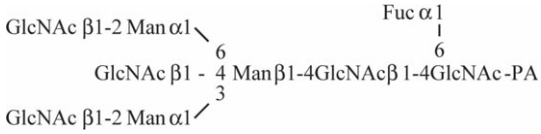 |
| (17) Ga-BA2 | 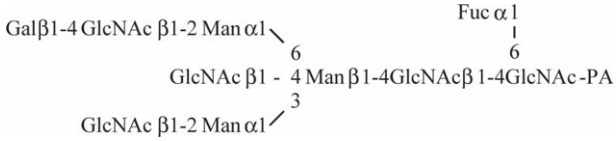 |
| (18) Gb-BA2 | 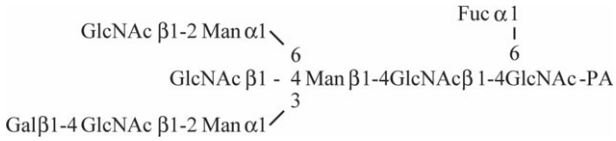 |
| (19) LewisXa-BA-2 | 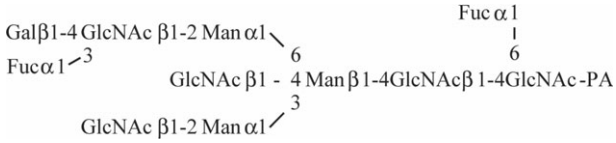 |
| (20) LewisXb-BA-2 | 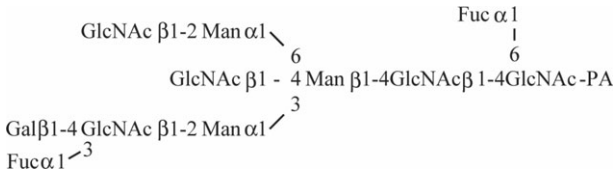 |
| (21) A2G2 | 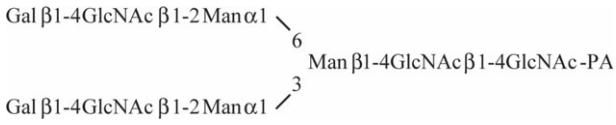 |
| (22) A2G2F | 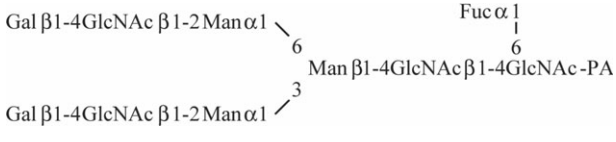 |
| (23) A2′G2F | 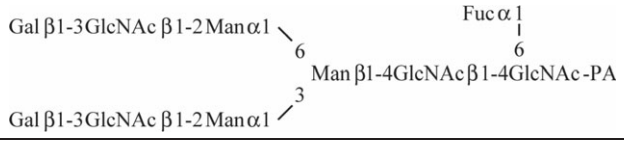 |

*Continued*

**Table II.** *Continued*

| Abbreviations | Structure |
|---|---|
| (24)A2G1Fo(6)G′1(3)F | 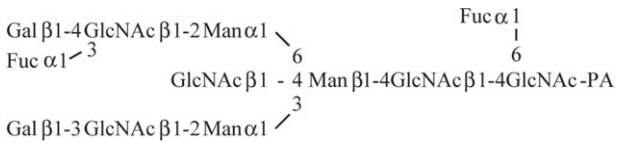 |
| (25) G2-BA-2 | 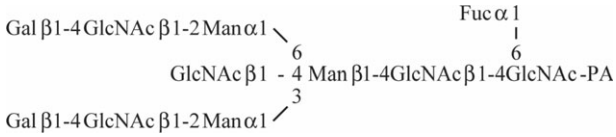 |
| (26) LewisX2-BA-2 | 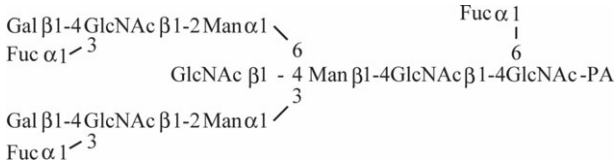 |
| (27) A2G1FoF | 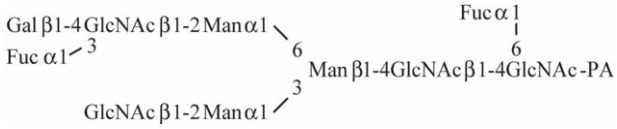 |
| (28) A3G3Fo2F | 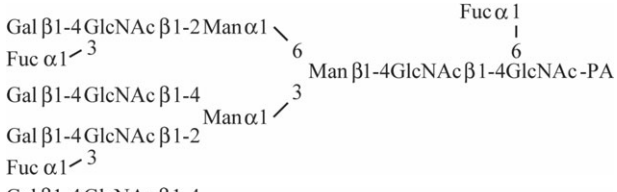 |
| (29) A4G4F | 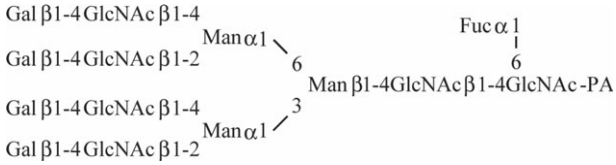 |

although its presence has been confirmed by the RT-PCR (S. Hitoshi and K. Ikenaka, unpublished results). One possible explanation that can account for this discrepancy is the presence of another (unidentified) fucosyltransferase that can synthesize core fucose residues. However, this was unlikely because *N*-linked sugar chains obtained from FuT VIII knockout mouse brain contained no core fucose residues (K. Ikenaka and N. Taniguchi, unpublished results). Our data fit with the previous report that the enzyme activity of FuT VIII does not correlate with mRNA levels in the brain (Miyoshi et al. 1997). This suggests that post-translational modifications or alternative mechanisms for FuT VIII activation may affect the enzymatic activity of FuT VIII.

BA-1 and BA-2 are *N*-linked sugar chains found predominantly in the brain that contains both bisecting GlcNAc and core fucose (Table II, Shimizu et al. 1993). Although the functions of most of the *N*-linked sugar chains, including BA-1 and BA-2, are unclear at present, there are several cases in which the role of sugar chains in the developing brain has been proposed. One such example is LewisX-BA-2 (combination of LewisXa-BA-2, LewisXb-BA-2, and LewisX2-BA-2). It was reported that the immunoreactivity of the rat monoclonal antibody L5 is associated with a complex-type *N*-linked sugar chain of glycoproteins, LewisX-BA-2 (Streit et al. 1996). The L5 epitope has been implicated in the outgrowth of astrocyte processes on an extracellular matrix component during postnatal development of mouse cerebellum (Streit et al. 1993; Streit and Stern, 1995). In the present study, we observed that the total amount of LewisX-BA-2 structure was low in E12, reaching its maximum at P7 in mouse cerebral cortex (Table III). We have also found that these sugar chains were mostly non-sialylated (data not shown). The increased level of LewisX-BA-2 was accompanied by a decrease in Gal-BA-2 (combination of Ga + Gb-BA-2 and G2-BA-2) level and an increase in BA-2 level (Table III). The biosynthetic pathway should proceed from BA-2 to Gal-BA-2 and to LewisX-BA-2 (Figure 3). It is also possible that Gal-BA-2 could be sialylated and become SialylGal-BA-2, which is actually present in the brain (data not shown). Therefore, it is reasonable to consider that the activity of β1,4-galactosyltransferase that adds galactose to BA-2 and the activity of sialyltransferase are high, while the activity of β1,3-fucosyltransferase that adds outer fucose to the Gal-BA-2 is low in the early embryo. Until now, FuT IV, VII and IX were known to be involved in the biosynthesis of LewisX or sialyl-LewisX; however, the expression of FuT IV

**Table III.** The expression profiles of *N*-glycans in mouse cerebral cortex.

| No. | Abbreviation | E12 | E16 | P0 | P7 | 12W |
|---|---|---|---|---|---|---|
| 1 | M9A | 10.2 | 6.8 | 5.5 | 5.5 | 4.7 |
| 2 | M8A | 11.2 | 7.4 | 6.9 | 7.7 | 4.7 |
| 3 | M7A | 3.8 | 2.9 | 3.0 | 3.1 | 2.0 |
| 4 | M7B | 2.6 | 1.9 | 2.1 | 2.9 | 2.5 |
| 5 | M6B | 9.9 | 8.5 | 8.3 | 8.0 | 7.6 |
| 6 | M5A | 7.6 | 12.4 | 14.7 | 16.8 | 23.5 |
| 7 | M4B | 1.3 | 1.0 | 1.1 | 0.8 | 0.5 |
| 8 | H5.1 | 0.4 | 0.8 | 1.0 | 0.7 | 0.6 |
| 9 | Lewis X-H4FB | <0.1 | 0.2 | 0.3 | 0.3 | 0.7 |
| 10 | A0G0 | 0.7 | 0.8 | 0.1 | 0.4 | 0.3 |
| 11 | Lewis X-H5F | 0.5 | 0.8 | 0.8 | 0.7 | 0.6 |
| 12 | A0G0F | 0.9 | 1.3 | 1.1 | 1.4 | 1.5 |
| 13 | A1(6)G0F | <0.1 | <0.1 | <0.1 | <0.1 | 0.3 |
| 14 | BA-1 | 0.3 | 0.3 | 0.3 | 0.6 | 4.2 |
| 15 | A2G0B | 0.4 | 0.4 | 0.6 | 0.8 | 0.9 |
| 16 | BA-2 | 1.8 | 3.6 | 4.6 | 5.3 | 4.3 |
| 17,18 | Ga + Gb-BA-2 | 2.2 | 1.2 | 1.4 | 1.3 | 0.7 |
| 19 | Lewis Xa-BA-2 | 1.0 | 2.1 | 3.0 | 4.5 | 2.2 |
| 20 | Lewis Xb-BA-2 | 0.4 | 0.8 | 1.3 | 1.1 | 1.5 |
| 21 | A2G2 | 0.2 | 1.8 | 1.7 | 0.7 | 0.3 |
| 22 | A2G2F | 4.1 | 2.5 | 2.0 | 2.4 | 1.1 |
| 23 | A2G'2F | <0.1 | <0.1 | 0.4 | 0.5 | 0.8 |
| 24 | A2G1Fo(6)G'1(3)F | <0.1 | <0.1 | <0.1 | 0.5 | 0.6 |
| 25 | G2-BA-2 | 4.9 | 1.4 | 0.6 | 0.3 | 0.1 |
| 26 | Lewis X2-BA-2 | 0.8 | 0.9 | 0.9 | 1.5 | 1.2 |
| 27 | A2G1FoF | <0.1 | <0.1 | <0.1 | 0.5 | 2.1 |
| 28 | A3G3Fo2F | <0.1 | <0.1 | <0.1 | <0.1 | 0.5 |
| 29 | A4G4F | 0.6 | 1.9 | 1.1 | 0.9 | 0.6 |
| | Total high-mannose type | 45.3 | 39.9 | 40.5 | 44.0 | 45.5 |
| | Total complex type | 18.1 | 18.7 | 19.4 | 22.5 | 22.9 |
| | Total hybrid type | 1.7 | 2.8 | 2.5 | 1.8 | 1.9 |
| | Core Fucose | 18.1 | 17.5 | 18.2 | 22.0 | 23.0 |
| | Outer Fucose | 3.1 | 5.1 | 6.6 | 9.2 | 9.4 |
| | Bisecting GlcNAc | 11.9 | 10.9 | 13.0 | 15.7 | 15.8 |
| | β1,3-Galactose epitope | <0.2 | 0.2 | 0.5 | 1.0 | 1.4 |

The nomenclature of the sugar chains is shown in "Abbreviations" and Table II. Numerical values represent the percentage of *N*-glycan.

and VII was below the detection limit in the cortex. The expression level of FuT IX was very low in E12, but increased significantly after E16, which is consistent with the developmental change in the LewisX-BA-2 sugar chain levels. From these results, it is suggested that FuT IX plays a major role in the biosynthesis of LewisX-BA-2 in the cerebral cortex.

On the other hand, none of the β1,4-galacosyltransferase genes were expressed at high levels at E12 (Table I). We are presently examining the galactosyltransferase responsible for galactosylating BA-2 (Nakakita et al. 1999), but its molecular nature remains unclear.

An interesting *N*-linked sugar chain expressed in the brain is BA-1, which does not contain a GlcNAc residue on the β1,3-Man branch (Table II). *N*-linked sugar chains with this structural feature are abundant in the brain (Chen et al. 1998), and we found that the level increases suddenly after P7 (Table III). In brain, hexosaminidase B removes the GlcNAc residue linked to the Man-β1,3 branch of BA-2 and converts BA-2 to BA-1 (Okamoto et al. 1999). The mRNA level of hexosaminidase B and the amount of BA-1 showed good correlation (Tables I and III), supporting the above conclusion. Since hexosaminidase is a lysosomal enzyme, it is possible that BA-1 is a degradation product. However, it was found in the highly purified myelin membrane fraction (data not shown) and therefore, it should be present on proteins present in the cell membrane.

### *Sugar chains containing β1,3-galactose residues*

In vertebrate, galactose is transferred either as α- or β-anomer through 1,3- or 1,4-linkage (Shur et al. 1998). By *N*-glycan expression analysis, we observed *N*-linked sugar chains containing Gal residues connected via β1,4 and β1,3-linkages (Table II). By macroarray analysis, the mRNA levels of β1,3-galactosyltransferase I, II, III were detected in P0, P7, and 12W cerebral cortices (Table I). These genes have been cloned and shown to be expressed in the brain (Hennet et al. 1998). While all were expressed at very low levels at E12, their expression increased after E16. This result is consistent with the change in the levels of β1,3 galactose-containing sugar chains (Table III).

## Conclusion

We have identified several *N*-linked sugar chains, the levels of which greatly change during development of the cerebral cortex. One of the sugar chain structures, LewisX-BA-2, was reported to exhibit function by itself. Thus, other developmentally regulated sugar chains may also have functions. To fully understand the functions of the sugar chains, it is important to determine the types of cells that express them. However, this will be a challenging task. Lectins or antibodies detect an epitope on the sugar chain and do not recognize the entire structure. In this respect, our present study suggests that the genes involved in their biosynthesis could assist in cell identification through in situ hybridization. We also suggested the presence of an unidentified enzyme: a β1,4-galactosyltransferase that adds galactose to BA-2. These represent intriguing targets for molecular cloning.

## Materials and methods

PA-sugar chains used as standard were purchased from Takara (Otsu, Japan) or Seikagaku Corporation (Tokyo, Japan). Neuraminidase derived from *Arthrobacter ureafaciens* was purchased from Nacalai Tesque (Kyoto, Japan). Hybond N, mRNA purification kit, Quick Prep Micro mRNA purification kit, and [α-$^{32}$P]dCTP were purchased from GE Healthcare (Buckinghamshire, UK). Trizol, Superscript II RNase H$^-$ Reverse Transcriptase and RNaseOUT, pZErO-2 vector, were purchased from Invitrogen (Carlsbad, CA). dATP, dCTP, dTTP, dGTP and *Taq* polymerase were purchased from Promega (Mannheim, Germany).

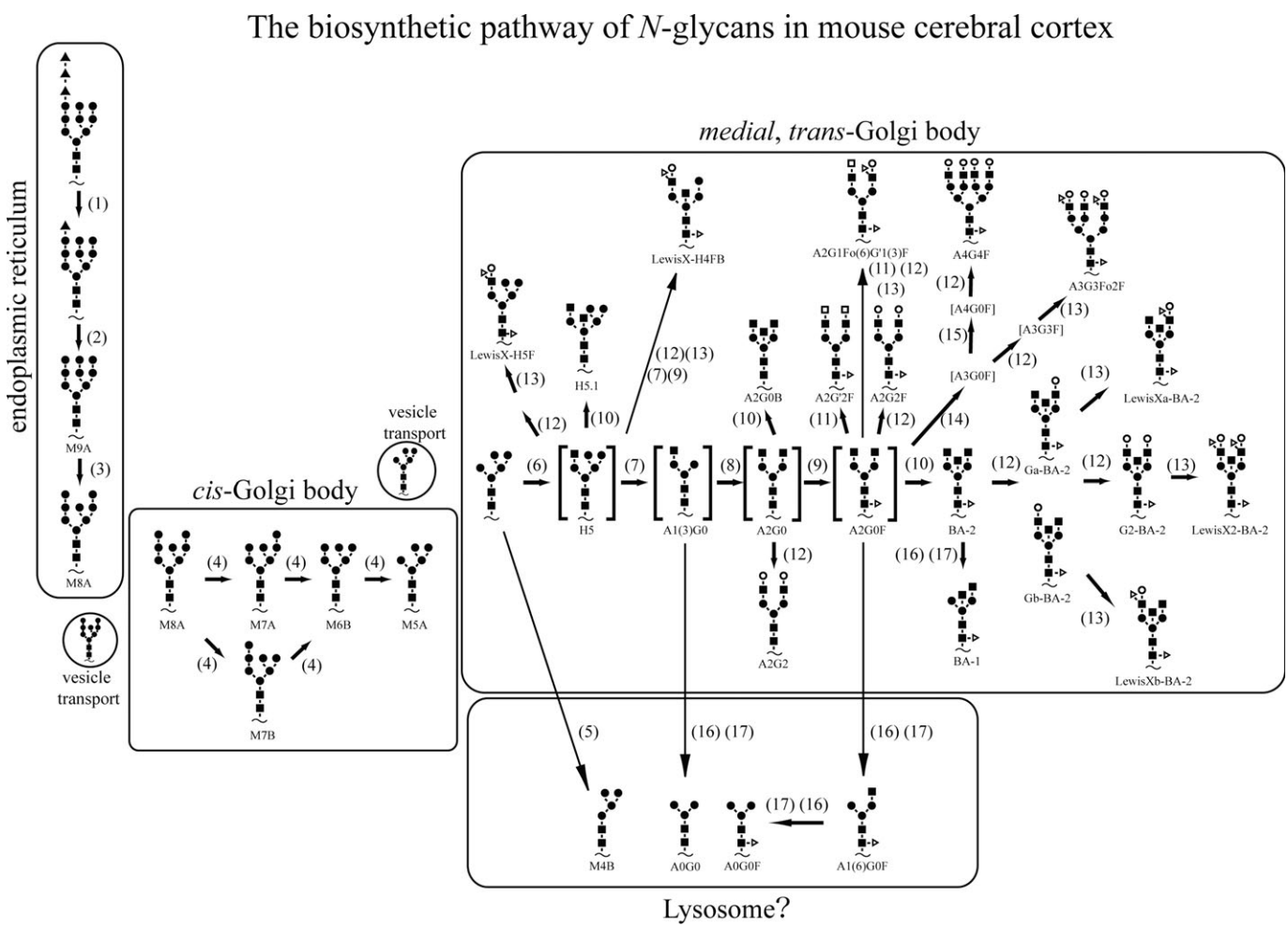


**Fig. 3.** Biosynthetic pathway of *N*-glycans in the mouse cerebral cortex. Relatively, few major *N*-linked sugar chains were detected in the cerebral cortex. Those biosynthetic pathways are depicted together with the enzymes catalyzing each biosynthetic pathway. Possible genes responsible for each pathway are shown in Table I. (1) glucosidase I, (2) glucosidase II, (3) ER α1,2-mannosidase, (4) Golgi-mannosidase IB, (5) lysosomal α-mannosidase, (6) *N*-acetylglucosaminyltransferase I, (7) mannosidase II, (8) *N*-acetylglucosaminyltransferase II, (9) fucosyltransferase VIII, (10) *N*-acetylglucosaminyltransferase III, (11) β1,3-galactosyltransferases I, II, III, (12) β1,4-galactosyltransferases II, III, V, VI, (13) fucosyltransferase IX, (14) *N*-acetylglucosaminyltransferase IV A, B, (15) *N*-acetylglucosaminyltransferase V, (16) hexosaminidase A, and (17) hexosaminidase B. ▲, glucose; •, mannose; ■, acetylglucosamine; ○, β1,4galactose; □, β1,3galactose; △, fucose; ∼, Protein.

*Array preparation*

*Cloning of target DNA*. The sequences of target cDNA were retrieved from the GenBank database (National Center for Biotechnology Information). Polyadenylated mouse RNA was isolated from embryonic (day 12) brain, liver, kidney, and adult (week 12) brain to synthesize cDNA. The mRNA was reverse transcribed with oligo ($dT_{17}$) primers and Superscript II reverse transcriptase as per the manufacturer's instructions. cDNA segments 500–2500 bp long without repetitive or polyadenylated sequences were chosen for the amplification by PCR reactions with primers that were synthesized by Oligotechnomart (Kyoto, Japan). The PCR products were subcloned into pZErO-2 plasmid vector and their sequences were confirmed by direct sequencing method. Sequencing of the 5′-end of the cDNA insert was performed with M13 forward or reverse primer using a DYEnamic ET Terminator Cycle Sequencing kit and ABI377 sequencer (Applied Biosystems, Foster City, CA). The following 28 cDNAs were purchased from Incytegenomics (St. Louis, MO): stroma factor 4, myosin Ib, hypoxanthine guanine phosphoribosyltransferase, ubiquitin B, tyrosine 3-monooxygenase, ribosomal protein S29, α-mannosidase (MAN2B2), lysosomal mannosidase, mannosidase IIx, α2,8-sialyltransferase 8D, α2,8-sialyltransferase 8B, sialyltransferase 7F, sialyltransferase 7c, sialyltransferase 7b, β-galactoside α2,6-sialyltransferase 1, sialyltransferase 4c, sialyltransferase 4, sialyltransferase 5, β1,3-galactosyltransferase II, β1,4-galactosyltransferase II, β1,4-galactosyltransferase V, α1,3-galactosyltransferase, polypeptide GalNAc transferase 1, polypeptide GalNAc transferase 3, glucosidase I, glucosidase II, acid α-glucosidase, and acid β-glucosidase. To amplify cDNA inserts for arraying, the same PCR primers used for cDNA cloning were used. For each cDNA clone, 5 ng of the plasmid DNA was used as a template in 50 μL PCR reaction containing 10 mM Tris–HCl (pH 8.3), 50 mM KCl, 1.5 mM $MgCl_2$, 0.1% Triton X-100, 12.5 μM of each primer, 0.2 mM dNTPs, and 3.25 U of *Taq* DNA polymerase. Amplification was done in a Peltier Thermal Cycler (MJ Research, MA)

under the following conditions: initial denaturation at 95°C for 2 min; then 35 cycles of denaturation at 94°C for 30 s, annealing at 60°C for 30 s, and extension at 72°C for 3 min; and then a final extension at 72°C for 7 min. PCR products were precipitated with ethanol, and the precipitates were washed with 70% ethanol and dissolved in TE buffer [10 mM Tris–HCl, 1 mM ethylenediaminetetraacetic acid (EDTA), pH 8.0] at a concentration of 2 μg/μL. To examine the quality and quantity of the PCR products, they were run on 1.2% agarose gels (Nacalai Tesque). The PCR products were mixed with 2× Array-BPB [4 mM Tris–HCl, pH 7.5, 0.4 mM EDTA, 24% (v/v) glycerol, 0.1% bromophenol blue] and transferred to a 384-well plate. The cDNAs were spotted onto the Hybond-N membranes (GE Healthcare) using a SPBIOII (Hitachi, Japan) or Microgrid II (Genomic Solutions, Ann Arbor, MI). A 48-pin gridding head (SPBIO II) or a 384-pin gridding head (Microgrid II) was used for spotting a grid of 384 spots. The spotted membranes were submerged in a denaturing solution (0.5 M NaOH, 1.5 M NaCl) and soaked for 1 min. The membranes were transferred into a neutralization solution (0.5 M Tris–HCl, pH 7.0, 1.5 M NaCl), soaked for 1 min and in 2× sodium chloride-sodium citrate buffer for 5 min. After drying, spotted PCR products on the membranes were cross-linked by ultraviolet light and baked for 30 min under vacuum at 80°C in a vacuum oven.

*mRNA purification.* Total RNA were extracted from ICR mice of various developmental stages (12-, 16-day fetal brain, P0 day, 7-day and 12-week postnatal brain, kidney, and liver), and the poly (A) RNA was isolated using Quick Prep Micro mRNA purification kit as per the manufacturer's instructions. The RNA concentration was quantitated by spectrophotometric analysis at 260 nm.

*Probe preparation*

An amount of 1 μg of poly (A) RNA was mixed with 1.8 μg of random primers in a total volume of 3.25 μL, heat denatured at 70°C for 5 min, and cooled on ice. A volume of 10 μL of [α-$^{32}$P] dCTP (3000 Ci/mmol), 1 μL of 0.1 M DTT, 5 μL of first-strand buffer (Invitrogen), 2 μL of dNTPs (10 mM each of dTTP, dGTP, and dATP and 37 μM dCTP), 20 U of RNaseOUT (Invitrogen), and 2 μL of Superscript II (Invitrogen) were added to the sample mixture. Each sample was incubated at 42°C for 1 h to synthesize $^{32}$P-labeled cDNA. After 1-h incubation, template RNA was degraded with 0.3 M NaOH at 65°C for 30 min, and the mixture was neutralized with 1 M Tris–HCl (pH 7.5). The $^{32}$P-labeled cDNA was purified on Sepharose-G50 column to eliminate unincorporated $^{32}$P-labeled nucleotides and very short synthetic cDNAs. The cDNA sample was fractionated into 10 eluates, and the eluates with the highest radioactivity were pooled and used for hybridization.

*Macroarray hybridization and data analyses*

Prehybridization of the cDNA macroarray membrane was performed in prehybridization solution [5× sodium chloride-sodium phosphate-EDTA buffer (SSPE), 50% (v/v) formamide, 5× Denhardt's solution, 0.5% (v/v) sodium dodecyl sulfate (SDS), 100 μg/mL herring sperm DNA] at 50°C for 4 h, and the membrane was rotated in 35 × 50 mm roller bottles. The purified probe was denatured in boiling water for 5 min and cooled on ice. Hybridization was performed by adding the denatured probe to the prehybridization solution and incubated at 50°C for 20 h in a roller oven. The membranes were washed twice in 2× SSPE, 0.1% SDS for 10 min at room temperature, followed by two washings in 1× SSPE, 0.1% SDS at 65°C for 20 min. After a final wash with 0.1× SSPE, 0.1% SDS for 20 min at 65°C, the membranes were exposed to a Fuji BAS-MS2325 intensifying screen for 7 days at 4°C. Then, the screen was scanned using a Fuji BAS 1800 II Phosphorimager (Fuji Photo Film Co., Ltd., Tokyo, Japan) at a maximum resolution of 50 μm. All the experiments were done in triplicate for each sample.

*Primer pairs and PCR conditions*

Template cDNAs for RT-PCR were synthesized from 200 ng of poly $(A)^+$ RNAs using 200 U Superscript II reverse transcriptase and random (N6) primers. PCRs were carried out using 0.25 U *Taq* DNA polymerase, 200 μM dNTP, 2 μM each primer set, and template cDNAs. PCR conditions were as follows: after incubation for 5 min at 96°C, 25–35 cycles of denaturing at 96°C for 45 s, annealing at 60°C for 45 s, extension at 72°C for 90 s, and final extension at 72°C for 7 min. The following oligonucleotide primers specific for mouse GnT III, ST8sia V, MIB, β1,3-galactosyltransferase I (β1,3GT1), FuT VIII, FuT IX, GAPDH were used.

GnT III:
5′-CCTCAAACTCTACGATGGCT-3′ (forward primer)
5′-CTACCCAGCCCTGTGAAAGTGCACA-3′ (reverse primer)

ST8sia V:
5′-ATGCGCTACGCAGACCCCT-3′ (forward primer)
5′-TCAGCAGCAATTGCAGGTGC-3′ (reverse primer)

MIB:
5′-GTAGGATACCACCTTTGAAC-3′ (forward primer)
5′-ACCAACTGATGTGTGATACT-3′ (reverse primer)

β1,3GT1:
5′-ATGGCTTCAAAGGTCTCCTG-3′ (forward primer)
5′-CTAACATCTCAGATGCTTCTTGCTT-3′ (reverse primer)

FuT VIII:
5′-CTATACTACCTCAGTCAAAC-3′ (forward primer)
5′-TATTTGACAAACTGGGACAC-3′ (reverse primer)

FuT IX:
5′-ACAACAAATCCCATGCGGTC-3′ (forward primer)
5′-GTGGGAATCAGATTTTTATC-3′ (reverse primer)

GAPDH:
5′-ATGGTGAAGGTCGGTGTGAACGGA-3′ (forward primer)
5′-TTACTCCTTGGAGGCCATGTAGGC-3′ (reverse primer)

*Pyridylamination of sugar chains released from tissue samples*

ICR mice of various developmental stages (E12, E16, P0, P7, 12W) were sacrificed, their cerebral cortices quickly removed and homogenized with nine volumes of acetone using a Polytron homogenizer. After placing on ice for 1 h, the

homogenate was centrifuged at 2150*g* for 20 min. The pellet was dried in a Spinvac centrifuge (TOMY, Tokyo, Japan). Acetone precipitated samples were subjected to manual hydrazinolysis, followed by *N*-acetylation, and pyridylaminated using the GlycoTag (Takara).

*Hydrazinolysis and N-acetylation*

A lyophilized sample (2 mg) was heated with 200-μL anhydrous hydrazine at 100°C for 10 h. Excess hydrazine was evaporated in vacuo. The remaining trace of hydrazine was removed by coevaporation with toluene several times. The released sugar chains were *N*-acetylated with freshly prepared sodium bicarbonate solution (saturated, 200 μL) and acetic anhydride (8 μL) by incubation on ice. Five minutes later, another 200 μL of bicarbonate solution and 8 μL of acetic anhydride were added. The reaction mixture was left to stand for 30 min on ice with occasional stirring. Dowex 50W-X2 (1 g, $H^+$ form, 100–200 mesh; Bio-Rad, Hercules, CA) was added to the solution to bring the pH to 3.0. The resin and the solution were poured into a Sepacol mini column™ (Seikagaku Corporation), and the column was washed with 5-fold bed volumes of distilled water. The flow-through fraction and the washings were combined, and concentrated to dryness by a rotary evaporator. A small amount of distilled water was added to the residue, and the solution was lyophilized in a conical tube and applied to the GlycoTag (Takara) for pyridylamination. Excess reagents were removed by extraction twice with 100-μL water-saturated phenol–chloroform mixture (1:1, v/v) followed by extraction with 100 μL chloroform and with 100 μL diethyl ether. After suspension of the lyophilized sample in 50 μL of distilled water, the sample was filtered using 0.2 μm low-binding hydrophilic polytetrafluroethylene membrane Ultrafree™ centrifugal filter (Millipore, Bedford, MA) before injection into HPLC columns.

*Sugar chain analysis by HPLC*

Pyridylaminated sugar chains were analyzed as previously described (Otake et al. 2001).

*Quantification of PA-sugar chains*

Digital chart recorder, Power Chrom™ (AD Instruments, Colorado Springs, CO) or MacIntegrator™ (Rainin Instruments, Woburn, MA) system running on Macintosh™ computers (Apple Computer, Cupertino, CA) were used for analysis of area and elution times of each peak. The amount of *N*-linked sugar chains contained in each tissue was quantified by adding the peak areas from all the fractions (M2–M11). The amount of each sugar chain was expressed as the molar percentage of the total *N*-linked sugar chains.

## Acknowledgments

We thank Dr. N. Ueno and Dr. A. Kitayama, Division of Morphogenesis, National Institute for Basic Biology for allowing us to use the cDNA macroarray spotting machine and their assistance with cDNA macroarray analysis. We thank Dr. A. Nishikawa, Department of Applied Biological Science, Tokyo University of Agriculture and Technology, for providing us GM9 PA sugar chain. We thank Dr. S. Tsuji for providing us sialyltransferase cDNAs and Prof. Steven Pfeiffer for his continuous encouragement.

## Conflict of interest statement

None declared.

## Abbreviations

β1,3GT1, β1,3-Galactosyltransferase I; cDNA, complementary deoxyribonucleic acid; 2D-HPLC, two-dimensional high-performance liquid chromatography; EDTA, ethylenediaminetetraacetic acid; FuT VIII, Fucosyltransferase VIII; FuT IX, Fucosyltransferase IX; GAPDH, glyceraldehyde-3-phosphate dehydrogenase; GnT III, *N*-acetylglucosaminyltransferase III; HPLC, high-performance liquid chromatography; MIB, Golgi mannosidase IB; mRNA, messenger ribonucleic acid; PA-sugar chain, pyridylamino-sugar chain; PCR, polymerase chain reactions; RT-PCR, reverse transcriptase-polymerase chain reaction; SDS, sodium dodecyl sulfate; SSPE, sodium chloride-sodium phosphate-EDTA buffer; ST8sia II, α2,8-sialyltransferase II; ST8sia V, α2,8-sialyltransferase V

## References

Amado M, Almeida R, Schwientek T, Clausen H. 1999. Identification and characterization of large galactosyltransferase gene families: galactosyltransferases for all functions. Biochim Biophys Acta. 1473:35–53.

Chen YJ, Wing DR, Guile GR, Dwek RA, Harvey DJ, Zamze S. 1998. Neutral *N*-glycans in adult rat brain tissue—complete characterization reveals fucosylated hybrid and complex structures. Eur J Biochem. 251: 691–703.

Comelli EM, Head SR, Gilmartin T, Whisenant T, Haslam SM, North SJ, Wong NK, Kudo T, Narimatsu H, Esko JD et al. 2006. A focused microarray approach to functional glycomics: transcriptional regulation of the glycome. Glycobiology. 16:117–131.

De Vries T, Knegtel RM, Holmes EH, Macher BA. 2001. Fucosyltransferases: structure/function studies. Glycobiology. 11: 119R–128R .

Dontenwill M, Roussel G, Zanetta JP. 1985. Immunohistochemical localization of a lectin-like molecule, R1, during the postnatal development of the rat cerebellum. Brain Res. 349:245–252.

Fujimoto I, Menon KK, Otake Y, Tanaka F, Wada H, Takahashi H, Tsuji S, Natsuka S, Nakakita S, Hase S et al. 1999. Systematic analysis of N-linked sugar chains from whole tissue employing partial automation. Anal Biochem. 267:336–343.

Geetha-Habib M, Noiva R, Kaplan HA, Lennarz WJ. 1988. Glycosylation site binding protein, a component of oligosaccharyl transferase, is highly similar to three other 57 kd luminal proteins of the ER. Cell. 54: 1053–1060.

Harduin-Lepers A, Mollicone R, Delannoy P, Oriol R. 2005. The animal sialyltransferases and sialyltransferase-related genes: a phylogenetic approach. Glycobiology. 15:805–817.

Helenius A, Aebi M. 2001. Intracellular functions of *N*-linked glycans. Science. 291:2364–2369.

Hennet T, Dinter A, Kuhnert P, Mattu TS, Rudd PM, Berger EG. 1998. Genomic cloning and expression of three murine UDP-galactose: beta-*N*-acetylglucosamine beta1,3-galactosyltransferase genes. J Biol Chem. 273:58–65.

Herscovics A. 1999. Importance of glycosidases in mammalian glycoprotein biosynthesis. Biochim Biophys Acta. 1473:96–107.

Jenkins N, Parekh RB, James DC. 1996. Getting the glycosylation right: implications for the biotechnology industry. Nat Biotechnol. 14:975–981.

Kemmner W, Roefzaad C, Haensch W, Schlag PM. 2003. Glycosyltransferase expression in human colonic tissue examined by oligonucleotide arrays. Biochim Biophys Acta. 1621:272–279.

Kono M, Yoshida Y, Kojima N, Tsuji S. 1996. Molecular cloning and expression of a fifth type of alpha2,8-sialyltransferase (ST8Sia V). Its substrate specificity is similar to that of SAT-V/III, which synthesize GD1c, GT1a, GQ1b and GT3. J Biol Chem. 271:29366–29371.

Kornfeld R, Kornfeld S. 1985. Assembly of asparagine-linked oligosaccharides. Annu Rev Biochem. 54:631–664.

Kuchler S, Rougon G, Marschal P, Lehmann S, Reeber A, Vincendon G, Zanetta JP. 1989. Location of a transiently expressed glycoprotein in developing cerebellum delineating its possible ontogenetic roles. Neuroscience. 33:111–124.

Kudo T, Ikehara Y, Togayachi A, Kaneko M, Hiraga T, Sasaki K, Narimatsu H. 1998. Expression cloning and characterization of a novel murine alpha1, 3-fucosyltransferase, mFuc-TIX, that synthesizes the Lewis x (CD15) epitope in brain and kidney. J Biol Chem. 273:26729–26738.

Menon K, Rasband MN, Taylor CM, Brophy P, Bansal R, Pfeiffer SE. 2003. The myelin-axolemmal complex: biochemical dissection and the role of galactosphingolipids. J Neurochem. 87:995–1009.

Miyoshi E, Uozumi N, Noda K, Hayashi N, Hori M, Taniguchi N. 1997. Expression of alpha1-6 fucosyltransferase in rat tissues and human cancer cell lines. Int J Cancer. 72:1117–1121.

Nakakita S, Menon KK, Natsuka S, Ikenaka K, Hase S. 1999. beta1-4Galactosyltransferase activity of mouse brain as revealed by analysis of brain-specific complex-type *N*-linked sugar chains. J Biochem. (Tokyo) 126:1161–1169.

Okamoto Y, Omichi K, Yamanaka S, Ikenaka K, Hase S. 1999. Conversion of brain-specific complex type sugar chains by *N*-acetyl-beta-D-hexosaminidase B. J Biochem. (Tokyo) 125:537–540.

Orlean P. 1992. Enzymes that recognize dolichols participate in three glycosylation pathways and are required for protein secretion. Biochem Cell Biol. 70:438–447.

Otake Y, Fujimoto I, Tanaka F, Nakagawa T, Ikeda T, Menon KK, Hase S, Wada H, Ikenaka K. 2001. Isolation and characterization of an *N*-linked oligosaccharide that is significantly increased in sera from patients with non-small cell lung cancer. J Biochem. (Tokyo) 129:537–542.

Schmitz B, Peter-Katalinic J, Egge H, Schachner M. 1993. Monoclonal antibodies raised against membrane glycoproteins from mouse brain recognize *N*-linked oligomannosidic glycans. Glycobiology. 3:609–617.

Shimizu H, Ochiai K, Ikenaka K, Mikoshiba K, Hase S. 1993. Structures of *N*-linked sugar chains expressed mainly in mouse brain. J Biochem. (Tokyo) 114:334–338.

Shur BD, Evans S, Lu Q. 1998. Cell surface galactosyltransferase: current issues. Glycoconj J. 15:537–548.

Spiro MJ, Spiro RG. 1991. Potential regulation of *N*-glycosylation precursor through oligosaccharide-lipid hydrolase action and glucosyltransferase-glucosidase shuttle. J Biol Chem. 266: 5311–5317.

Streit A, Stern CD. 1995. L5: a carbohydrate epitope involved in neural development. Biol Cell. 84:63–67.

Streit A, Nolte C, Rasony T, Schachner M. 1993. Interaction of astrochondrin with extracellular matrix components and its involvement in astrocyte process formation and cerebellar granule cell migration. J Cell Biol. 120: 799–814.

Streit A, Yuen CT, Loveless RW, Lawson AM, Finne J, Schmitz B, Feizi T, Stern CD. 1996. The Le(x) carbohydrate sequence is recognized by antibody to L5, a functional antigen in early neural development. J Neurochem. 66:834–844.

Taniguchi N, Honke K, Fukuda M (editors). 2002. Handbook of Glycosyltransferases and Related Genes. Tokyo: Springer

Ten Hagen KG, Fritz TA, Tabak LA. 2003. All in the family: the UDP-GalNAc:polypeptide *N*-acetylgalactosaminyltransferases. Glycobiology 13:1R–16R.

Yoshida Y, Kojima N, Kurosawa N, Hamamoto T, Tsuji S. 1995. Molecular cloning of Sia alpha 2,3Gal beta 1,4GlcNAc alpha 2,8-sialyltransferase from mouse brain. J Biol Chem. 270:14628–14633.